Earthq Eng & Eng Vib (2015) 14: 487-502 **DOI**:10.1007/s11803-015-0039-9

A comparative study of semi-active control strategies for base isolated buildings

Oliveira F.[1†], Morais P.[1‡] and Suleman A.[2§]

1. *National Laboratory for Civil Engineering (LNEC), Av. do Brasil 101, 1700-066 Lisbon, Portugal*

2. *University of Victoria, Dep. Mechanical Engineering, PO Box 1700, Stn CSC, Victoria, BC, V8W 2Y2, Canada*

Abstract: A comparative analytical study of several control strategies for semi-active (SA) devices installed in base-isolated buildings aiming to reduce earthquake induced vibrations is presented. Three force tracking schemes comprising a linear controller plus a "clipped" algorithm and a nonlinear output feedback controller (NOFC) are considered to tackle this problem. Linear controllers include the integral controller (I), the linear quadratic regulator (LQR) and the model predictive controller (MPC). A single degree-of-freedom system subjected to input accelerograms representative of the Portuguese seismic actions are first used to validate and evaluate the feasibility of these strategies. The obtained results show that structural systems using SA devices can in general outperform those equipped with passive devices for lower fundamental frequency structural systems, namely base-isolated buildings. The effectiveness of the proposed strategies is also evaluated on a 10 storey base-isolated dual frame-wall building. The force tracking scheme with an integral controller outperforms the other three as well as the original structure and the structure equipped with passive devices.

Keywords: semi-active control; integral controller; linear quadratic regulator; predictive control; nonlinear output feedback control; seismic hazard mitigation; hybrid base-isolation.

1 Introduction

Structures such as hospitals, energy power stations, communication centres, and civil protection and fire station buildings are vital to be kept operational during and immediately after the occurrence of an earthquake. With this concern, new concepts for vibration control of structures when subjected to earthquakes have been proposed in recent years based on passive, semi-active (SA), active and hybrid vibration control systems (Casciati *et al*., 2012; Chu *et al*., 2005; Ikeda, 2009; Soong and Dargush, 1997; Soong and Spencer Jr., 2002; Spencer Jr. and Nagarajaiah, 2003).

The base isolation concept has been commonly considered for reducing the transmission of seismic forces and energy to the main structure. The goal consists in decoupling the structure (superstructure) from the foundation in order to reduce the potential for structural damage and increase equipment safety due to the earthquake ground motions (Chopra, 1995). However base isolation systems present some drawbacks. One is the increase of the isolation displacement beyond the operational design range under large pulse-like ground motions generated at near fault locations. Thus, supplementary devices (damping systems) are often prescribed or suggested to reduce isolator displacements without increasing superstructure response (Gavin and Aldemir, 2005). Hybrid systems combining base-isolated structures with semi-active systems have been receiving much attention in recent years as an alternative to passive systems (Bahar *et al*., 2010; Gavin and Aldemir, 2005; Luo *et al*., 2001). Magneto-rheological (MR) and fluid viscous dampers (FVD) are typical semi-active devices considered in these situations (Chu *et al*., 2005; Soong and Spencer Jr., 2002; Spencer Jr. and Nagarajaiah, 2003; Symans and Constantinou, 1999).

Semi-active control in particular has received considerable attention in recent years due to the advantages of offering similar reliability to passive control devices and maintaining the adaptability of active control systems with low power requirements. The idea of changing the damping characteristics in real

Correspondence to: Afzal Suleman, University of Victoria, Dep. Mechanical Engineering, PO Box 1700, Stn. CSC, Victoria, BC, V8W 2Y2, Canada
Tel: +1 250-721-6039; Fax: +1 250 721 6051
E-mail: suleman@uvic.ca
[†]Scholarship Holder, PhD Candidate, MSc; [‡]Researcher, PhD; [§]Professor, PhD, PEng

Supported by: The Portuguese Foundation for Science and Technology (FCT) for the PhD scholarship provided (reference SFRH/BD/84769/2012)
Received July 18, 2014; **Accepted** November 25, 2014

time between an upper and a lower limit has been studied by several researchers (Symans and Constantinou, 1999). An extensive analytical and experimental study was conducted by Symans and Constantinou (1995) where two semi active fluid dampers (two-stage damper and a variable fluid damper) on two structural models (one-storey structure and a three-story structure with fundamental periods of 0.36 s and 0.56 s) subjected to different seismic excitations were tested. They found results comparable to those of a passive control system with high damping. One analytical study covering different structural periods (from 0.2 s to 3 s) was made later on by Sadek and Mohraz (1998), which states that variable dampers with an adequate algorithm can be effective in reducing the acceleration responses of flexible structures. During the 90′s MR dampers gained attention due to their high dynamic range, low power requirements and large force capacity. Dyke and Spencer Jr. (1997) evaluated the effectiveness of this technology in civil engineering applications and found results better than the passive solution. After that a lot of analytical and experimental work has been performed to demonstrate the effectiveness this technology (Shook *et al.*, 2007; Qin *et al.*, 2008; Gattulli *et al.*, 2009; Mehrparvar and Khoshnoudian, 2012; Bharti *et al.*, 2014).

The use of semi-active devices for vibration control of structures leads to a nonlinear system (structure plus device) with bounded inputs. The analysis and design of nonlinear systems can be made using a number of available procedures. Ou and Li (2009) proposed design approaches for active, semi-active and passive control systems based on analysing the characteristics of the active control force. In general it is intended to derive feedback control laws that force the closed loop to follow the specifications. Several methods have been used for semi-active control: (i) Lyapunov based methods (Dyke and Spencer Jr., 1997; Jansen and Dyke, 2000; Luo *et al*., 2001); (ii) maximum energy dissipation algorithm and the modulated homogeneous friction algorithm (Dyke and Spencer Jr., 1997; Jansen and Dyke, 2000; Jung *et al.*, 2006); (iii) sliding mode control (Komatsu *et al.*, 2007; Symans and Constantinou, 1995); (iv) quantitative feedback theory and backstepping control technique (Zapateiro *et al.*, 2010); (v) intelligent paradigms, like neural networks or fuzzy-logic (Shook *et al.*, 2007); and (vi) force-tracking. The last one has been successfully applied in semi-active control and comprises different control schemes: force feedback and model-based feed-forward. In both cases the controller is designed to derive a desired force, e.g. optimal control (Dyke and Spencer Jr., 1997; Gavin and Aldemir, 2005; Jansen and Dyke, 2000; Sadek and Mohraz, 1998; Shook *et al.*, 2007), proportional plus integral control (Aguirre *et al*., 2011) or the force derivative feedback control (Rodríguez *et al*., 2012), which is converted in the control variable by using a bang-bang rule taking into account the measured force by the device (force feedback) or, using the inverse model of the device when it is possible (model-based feed-forward).

From a practical application perspective, the first application of semi-active fluid dampers in a base-isolated structure was made in 2000, the House of Creation and Imagination of Keio University - Yokohama (Ikeda, 2009). Another application was made later (2005) in the 11-storey of Keio University building - Mita South Building (Komatsu *et al.*, 2007). In the realm of MR devices, the first application was made in 2001 on the Nihon-Kagaku-Miraikan, the Tokyo National Museum of Emerging Science and Innovation, with two 30 t MR fluid dampers installed between the third and fifth floors (Spencer Jr., 2008). Also in Japan, a base-isolated building consisting of 40 t MR dampers along with laminated rubber bearings, lead dampers and oil dampers was constructed for residential use (Spencer Jr. and Nagarajaiah, 2003).

In this paper, semi-active control of base-isolated structures under several earthquake ground motions is investigated. Several control strategies are examined and the control effectiveness is evaluated for different controller gains and compared with the best passive case. A brief description of the research method is given first, then the models and control strategies are described, and finally a numerical analysis is carried out to evaluate their performance. The experience accumulated in designing semi-active systems can be used to implement and deliver this technology.

2 Analysis method

In this work four control strategies are investigated to drive semi-active devices for reducing structural responses, with special emphasis on base-isolated buildings. Three force tracking schemes and a nonlinear output feedback control strategy are evaluated numerically and compared. For the force tracking schemes, the integral controller, the linear quadratic regulator and the model predictive controller are considered to derive a desired force, which is used to compute the control variable for the device using an algorithm. Two algorithms are considered to “clip” the control variable: the inverse model of the damper and an on-off algorithm. The Maxwell model is adopted as a general way to model the transient and stationary regime of SA devices. A single degree of freedom (SDOF) mechanical model is adopted to analyse the applicability of these strategies in structures. Several earthquake ground motions (near- and far-field) for the Portuguese territory have been considered in the analysis. A methodology to tune the controller using the structural system model and the seismicity of the site is considered. Comparisons with the original structure and with the structure equipped with passive devices are made. A numerical example of a typical 10-storey

base-isolated building (multi degree of freedom model – MDOF) is considered for performance evaluation.

3 Hybrid base-isolated structure

For the purpose of this study a hybrid base-isolated building consisting of a superstructure constructed over a base floor supported by bearings with devices installed at the base level is considered. In this work both superstructure and bearings are described by linear models. The hybrid base-isolated structure is described by the mass $\boldsymbol{M}_s$, stiffness $\boldsymbol{K}_s$ and damping $\boldsymbol{C}_s$ matrices and is subjected to input disturbances (earthquake) $\ddot{x}_g$ and input forces f developed by additional devices at the base level. The model for an n degree of freedom system (base plus n-1 floors) is described in terms of the relative coordinates to the ground ($\boldsymbol{x}_{rg}$, $\dot{\boldsymbol{x}}_{rg}$ and $\ddot{\boldsymbol{x}}_{rg}$ as the vectors of relative displacements, velocities and accelerations) as:

$$\boldsymbol{M}_s \cdot \ddot{\boldsymbol{x}}_{rg} + \boldsymbol{C}_s \cdot \dot{\boldsymbol{x}}_{rg} + \boldsymbol{K}_s \cdot \boldsymbol{x}_{rg} = -\boldsymbol{M}_s \cdot \boldsymbol{1} \cdot \ddot{x}_g + \boldsymbol{G} \cdot f \quad (1)$$

where: $\boldsymbol{1}$ is a unitary column vector; and $\boldsymbol{G} = [-1\ 0 \ldots 0]^T$ is the matrix that defines the input force location. The system described in Eq. (1) can be represented in the state-space form by:

$$\dot{\boldsymbol{z}} = \boldsymbol{A} \cdot \boldsymbol{z} + \boldsymbol{B} \cdot f + \boldsymbol{E} \cdot \ddot{x}_g, \quad \boldsymbol{y} = \boldsymbol{C} \cdot \boldsymbol{z} + \boldsymbol{D} \cdot f$$

$$\boldsymbol{A} = \begin{bmatrix} \boldsymbol{0} & \boldsymbol{I} \\ -\boldsymbol{M}_s^{-1} \cdot \boldsymbol{K}_s & -\boldsymbol{M}_s^{-1} \cdot \boldsymbol{C}_s \end{bmatrix}, \ \boldsymbol{B} = \begin{bmatrix} \boldsymbol{0}_{nx1} \\ \boldsymbol{M}_s^{-1} \cdot \boldsymbol{G} \end{bmatrix}, \ \boldsymbol{E} = \begin{bmatrix} \boldsymbol{0}_{nx1} \\ -\boldsymbol{1} \end{bmatrix} \quad (2)$$

where $\boldsymbol{z} = \left\{ \boldsymbol{x}_{rg}, \dot{\boldsymbol{x}}_{rg} \right\}^T$ is the state vector; $\boldsymbol{C}$ and $\boldsymbol{D}$ are defined accordingly to the quantities for output; for instance if $\boldsymbol{C} = \boldsymbol{A}$ and $\boldsymbol{D} = \boldsymbol{B}$ the system outputs will be the relative velocities and absolute accelerations; $\boldsymbol{0}$, $\boldsymbol{0}_{nx1}$, $\boldsymbol{I}$ and $\boldsymbol{1}$ are a null matrix, null vector, identity matrix and unitary vector respectively.

Additional devices can be installed between the ground floor and the base floor. These devices can be passive, semi-active or active. Semi-active devices are considered and a general parametric model to describe the transient and stationary regime is used. The transient regime is related with the device time response, the time to develop the device force (stationary regime) after input the command to change its characteristics is given. It is dependent on the behaviour of each component of the device, for example: controller driving current, electrovalves, device type, and other components. This time response, also referred as the total time delay, can be described as the sum of pure time delays (or dead time) and lag (or phase delay), which are also designated as static and dynamic response time respectively (Symans and Constantinou, 1995). Time delays can change during operation (as the control variable increases or decreases) and an average time delay considering both operation processes is usually taken. In this work the device total time response (or delay) is accounted as lag and a first order dynamic system is considered to model the transient regime. In what concerns to the stationary regime, each device is represented by a specific model depending on the type of device used, which describes the energy dissipated. MR dampers and FVD are typical examples of semi-active devices described by specific mathematical models (Soong and Spencer Jr., 2002; Symans and Constantinou, 1999; Wang and Liao, 2011). The energy dissipation mechanism is modelled in this work by the classical dashpot model with an equivalent damping value. Thus, the device model is thus represented by the classical Maxwell model:

$$T_d \cdot \dot{f} + f = c_v \cdot \dot{x}_r, \ c_{min} \le c_v \le c_{max} \quad (3)$$

where: T_d is the relaxation time (or time lag); f is the damping force; c_v is the damping coefficient (time dependent) which can be changed between a minimum c_{min} and a maximum c_{max} value; and $\dot{x}_r$ is the relative velocity between the cylinder case and the piston head of the damper.

4 Semi-active control

The control problem can be established using the structure model (2) and the device model (3), which results in a new state-space system. This system has an augmented state-vector $\boldsymbol{z}_c = \{\boldsymbol{z}, f\}^T$, the ground motion $\ddot{x}_g$ as an input disturbance, and the device damping coefficient c_v as the control variable. The model and the corresponding matrices are given by:

$$\dot{\boldsymbol{z}}_c = \boldsymbol{A}_c \cdot \boldsymbol{z}_c + \boldsymbol{g}(\boldsymbol{z}_c) \cdot c_v + \boldsymbol{E}_c \cdot \ddot{x}_g, \quad \boldsymbol{y} = \boldsymbol{C}_c \cdot \boldsymbol{z}_c$$

$$\boldsymbol{A}_c = \begin{bmatrix} \boldsymbol{A} & \boldsymbol{B} \\ \boldsymbol{0} & -1/T_d \end{bmatrix}, \ \boldsymbol{g}(\boldsymbol{z}_c) = \begin{bmatrix} \boldsymbol{0}_{2nx1} \\ \dot{x}_r / T_d \end{bmatrix}, \ \boldsymbol{E}_c = \begin{bmatrix} \boldsymbol{E} \\ 0 \end{bmatrix} \quad (4)$$

where: $\boldsymbol{A}_c$, $\boldsymbol{E}_c$ and $\boldsymbol{C}_c$ are the new system matrices; $\boldsymbol{g}(\boldsymbol{z}_c)$ is the input vector dependent of the states (relative velocity). The system in Eq. (4) is a nonlinear dynamical system subjected to input disturbances with bounded control variable (input damping: $c_{min} \le c_v \le c_{max}$). The goal is to find the damping coefficient c_v (inside the admissible region) that minimizes the system structural accelerations and relative displacements. Using the available information from measurements, different

control approaches were used to compute the damping coefficient (Fig. 1). Those approaches are classified into: (i) force tracking scheme; (ii) and a nonlinear output feedback control strategy.

For implementation of the control strategies and establishment of the control laws, a single degree-of-freedom SDOF approach of the structural model in (1) was considered. This approach results from the fact that base-isolated structures first vibration mode (pole nearest the imaginary axis) will dominate the transient-response behaviour (the ratios of the poles real part exceed five and there are no zeros nearby), and thus are called dominant poles (Ogata, 1970). Moreover, it is well accepted that the movement of the superstructure can be considered similar to the one of a rigid body when a base isolation system is used since the interaction forces (damping and elastic forces developed between the base and first floor) will be small in comparison with the rest of the forces acting on the base (Luo *et al*., 2001; Rodríguez *et al*., 2012). Thus, the SDOF system is described by the total structure mass m and the characteristics of the isolation interface, stiffness k_b and damping c_b, which in terms of modal quantities is described by the natural frequency $\omega_b = \sqrt{k_b / m}$ and the damping ratio $\xi_b = c_b / (2 \cdot m \cdot \omega_b)$. The SDOF system can be described by the model in Eqs. (1) and (2) with the following equalities: $\boldsymbol{M}_s = m$; $\boldsymbol{C}_s = c_b$; $\boldsymbol{K}_s = k_b$; $\mathbf{G} = -1$; $\boldsymbol{x}_{rg} = x_{0g}$; $\dot{\boldsymbol{x}}_{rg} = \dot{x}_r = \dot{x}_{0g}$; $\ddot{\boldsymbol{x}}_{rg} = \ddot{x}_{0g}$; $\boldsymbol{z} = \left\{x_{0g}, \dot{x}_{0g}\right\}^T$. With this model the responses are given at the base floor only. This system is output (absolute base acceleration) and state (relative displacement and velocity) controllable since the correspondent controllability matrices $\boldsymbol{C}_o$ and $\boldsymbol{C}_s$ have full rank (Ogata, 1970):

$$\begin{gathered}\boldsymbol{C}_o = \left[\boldsymbol{C}\cdot\boldsymbol{B} \mid \boldsymbol{C}\cdot\boldsymbol{A}\cdot\boldsymbol{B} \mid \boldsymbol{D}\right], \boldsymbol{C}_s = \left[\boldsymbol{B} \mid \boldsymbol{A}\cdot\boldsymbol{B}\right] \\ \boldsymbol{A} = \begin{bmatrix} 0 & 1 \\ -k_b / m & -c_b / m \end{bmatrix}, \boldsymbol{B} = \begin{bmatrix} 0 \\ -1/m \end{bmatrix}, \\ \boldsymbol{C} = \left[-k_b / m \;\; -c_b / m\right], \boldsymbol{D} = -1/m\end{gathered} \tag{5}$$

Thus, it is possible to move those variables from one value to another using a control force f within some finite time window.

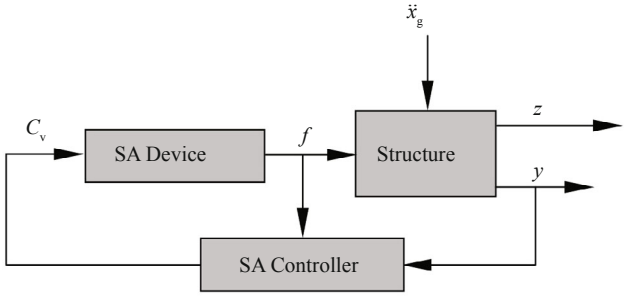

Fig. 1 Hybrid system closed-loop block diagram

4.1 Force tracking schemes

Force tracking schemes (Fig. 2) comprise a linear controller and a control algorithm. In this work the following controllers (Section 4.1.1 to 4.1.3) were considered to compute the desired force f_d using the output measurements $\boldsymbol{y}$ from the structure: the Integral control law (I), the linear quadratic regulator (LQR) and a model predictive control strategy (MPC). In order to adjust the device damping two approaches are used (Section 4.1.4 and 4.1.5): i) model-based feed-forward force tracking scheme where a variable damping (VD) algorithm is used to compute the device damping using the information resulting from the controller (desired force f_d); ii) force feedback where a clipped on-off (COO) algorithm is used, which also makes use of the measured force. The resulting force tracking schemes will be referred as: I VD; I COO; LQR VD; LQR COO; MPC VD; and MPC COO.

4.1.1 Integral control law

This control law is the well known integral control action used in industrial automatic controllers (Ogata, 1970). In vibration isolation problems it is commonly known as the sky-hook damper or absolute velocity feedback (Preumont, 2002). The SA device (force generating element) is installed together with a sensor at the base floor, which by using an integral control law is able to compute the desired control action f_d which is given as:

$$f_d = g \int_0^\tau \ddot{x}_0 \, \mathrm{d}\tau = g \cdot \dot{x}_0 \tag{6}$$

where: g is the controller gain; $\ddot{x}_0$ and $\dot{x}_0$ are the absolute acceleration and velocity at the base floor respectively. The controller gain for a specific system damping ratio $\xi = \xi_b + \xi_a$ is given by:

$$g = 2 \cdot m \cdot \omega_b \cdot (\xi - \xi_b) \tag{7}$$

where: $\xi_a = g / (2 \cdot m \cdot \omega_b)$ is the damping ratio provided by the integral controller. Controller gains g should be chosen in order to guarantee a stable closed-loop system. For the SDOF model considered in the

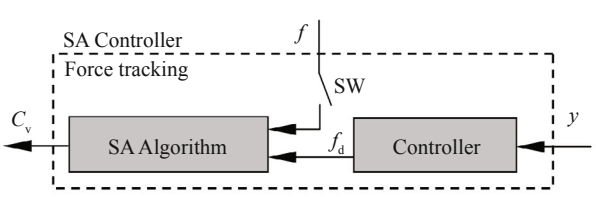

Fig. 2 SA controller using a force tracking scheme: (i) SW off – model-based feed-forward force tracking scheme; (ii) SW on – force feedback

controller formulation and the above integral control law the following transfer function in terms of absolute accelerations, which accounts for the effects of the external disturbances (earthquake ground motion) on the acceleration, is obtained:

$$\frac{A_0}{A_g} = \frac{c_b \cdot s + k_b}{m \cdot s^2 + (c_b + g) \cdot s + k_b} \tag{8}$$

where: A_0 and A_g are the Laplace transforms of $\ddot{x}_0$ and $\ddot{x}_g$ respectively; and s is the complex variable. Thus, stable solutions are found if all the poles lie in the left-half s plane. Moreover, from Eq. (8) it is found that the increase of damping provided by the controller gain does not influence the acceleration higher frequency attenuation (roll-off) as it happens with a constant damping system.

Having the structure characterized it is possible to design the controller gain g for a given damping ratio ξ. Some hints to derive the controller gain as function of the system desired damping ratio can be found in several references (Ogata, 1970; Skogestad and Postlethwaite, 1996; Preumont, 2002), mostly agreeing that the desired damping should be specified in a broad range of values: $0.4 \le \xi \le 1$. In this work the controller gain was achieved through numerical simulations considering a representative sample of input ground motions (accelerograms) of the site were the structure is to be installed and select the gain (or damping) that minimizes the mean peak acceleration responses.

4.1.2 Linear quadratic regulator

The so-called linear quadratic regulator was considered to derive the desired force for the SA algorithm. Assuming that the system is subjected to white noise excitation $w = \ddot{x}_g$, with zero mean $E[w] = 0$ and co-variance $E[w \cdot w^T] = W$, the performance index that weights the output $\boldsymbol{y} = \ddot{x}_0$ (base floor acceleration described in the state-space model by $\boldsymbol{C} = \{-k_b/m, -c_b/m\}$ and $\boldsymbol{D} = \{-1/m\}$, and weights the input desired force f_d is given by:

$$J = \lim_{\tau \to \infty} \frac{1}{\tau} E\left\{ \int_0^{\tau} \left(q \cdot \ddot{x}_0^2 + r \cdot f_d^2 \right) \mathrm{d}t \right\} \tag{9}$$

where: q and r are the weighting values on the output and input respectively; and $E\{\cdot\}$ is the expectation operator. The solution of this problem will lead to a linear control law function of the states $\boldsymbol{z}$, which is found considering the time invariant and steady-state solution given by a constant gain matrix $\boldsymbol{K}_y$ (Anderson and Moore, 1989):

$$f_d = -\boldsymbol{K}_y \cdot \boldsymbol{z}, \;\; \boldsymbol{K}_y = \boldsymbol{R}^{-1}\left[\boldsymbol{B}^T \cdot \boldsymbol{P} + \boldsymbol{N}^T \right] \tag{10}$$

where: $\boldsymbol{R} = r + q/m^2$; and $\boldsymbol{N} = q \cdot \{k_b/m^2, c_b/m^2\}^T$. Matrix $\boldsymbol{P}$ can be found by solving the following *Riccati* equation:

$$\boldsymbol{P}\boldsymbol{A} + \boldsymbol{A}^T\boldsymbol{P} - (\boldsymbol{P}\boldsymbol{B} + \boldsymbol{N})\boldsymbol{R}(\boldsymbol{B}^T\boldsymbol{P} + \boldsymbol{N}^T) + q\boldsymbol{C}^T\boldsymbol{C} = 0 \tag{11}$$

Adequate controller solutions should be stable in closed-loop (linear counterpart, considering $f = f_d$). Substituting Eq. (10) in Eq. (2), the closed-loop system is found:

$$\dot{\boldsymbol{z}} = \left(\boldsymbol{A} - \boldsymbol{B} \cdot \boldsymbol{K}_y \right) \cdot \boldsymbol{z} + \boldsymbol{E} \cdot \ddot{x}_g \tag{12}$$

Thus, controller gains $\boldsymbol{K}_y$ should be chosen such that the dynamic matrix $(\boldsymbol{A}\text{-}\boldsymbol{B}\cdot\boldsymbol{K}_y)$ eigenvalues have negative real part.

With the presented formulation a preliminary analysis was made in order to identify the weights that are more beneficial for the system response. A unitary input weighting value $r = 1$ s/kg was considered and the output weight q was tuned through numerical simulations considering a representative sample of input ground motions (accelerograms) in order to identify the value that minimizes the mean peak acceleration responses.

4.1.3 Model predictive controller

A predictive control strategy was also considered to derive the desired force. The idea behind this controller consists in predicting future outputs from actual measurements and past inputs using the system model (predictor), compare those outputs with the reference output (base floor acceleration) values, which is set to zero, and determine input trajectories that result from the solution of an optimization problem (optimizer). The prediction model used in the controller formulation considers input delays resulting from the input action f generated by the device due to the device time response (described by T_d). Thus, the formulation takes into account that the desired force f_d computed at time t-T_d will result in a force f applied by the device on the structure at time t. Since the controller is formulated in discrete-time domain, the following relationship holds: $f(k) = f_d(k\text{-}d)$, where the index k counts the time steps resulting from the discretisation process with a sampling time T_s, and $d = T_d/T_s$. Measurement delays are assumed to be small when compared to the input delays and thus are not considered in the formulation. It is also assumed that the controller computes the input during the control interval T_s (or sampling period). Under these assumptions, the structural model described by Eq. (2) for the SDOF case with input time delays, results in the following discrete-time domain controller internal model:

$$\begin{aligned} \boldsymbol{z}_a(k+1) &= \boldsymbol{A}_a \cdot \boldsymbol{z}_a(k) + \boldsymbol{B}_a \cdot f_d(k) + \boldsymbol{E}_a \cdot a_g(k) \\ \boldsymbol{y}(k) &= \boldsymbol{C}_a \cdot \boldsymbol{z}_a(k) \end{aligned} \tag{13}$$

where: $\boldsymbol{z}_a = \{z(k), f_d(k\text{-}d), \ldots, f_d(k\text{-}1)\}^T$ is the state vector, including the relative displacement and velocity at the base and the past instant desired forces $f_d(k\text{-}i)$, $i = 1,2\ldots d$

(dimension (2+d)×1); $f_d(k)$ is the actual desired force (scalar); $a_g(k)$ is the input ground motion (scalar); the output vector $\boldsymbol{y}(k) = a(k)$ is the base floor acceleration (scalar); and $\boldsymbol{A}_a$, $\boldsymbol{B}_a$, $\boldsymbol{E}_a$ and $\boldsymbol{C}_a$ are the discretized state-space model matrices. Using this model to predict future outputs in a specific prediction horizon (HP steps), the vector of output predictions $\boldsymbol{Y}$ is given as (Maciejowski, 2002):

$$\begin{aligned}\boldsymbol{Y}(k) = \boldsymbol{\Psi}\cdot\hat{\boldsymbol{z}}_a(k\,|\,k) + \boldsymbol{\Theta}\cdot f_d(k-1) \\ + \boldsymbol{\Theta}\cdot\Delta f_d(k) + \boldsymbol{\Xi}\cdot\boldsymbol{A}_g(k)\end{aligned} \tag{14}$$

where: $\boldsymbol{Y}(k) = \{\hat{y}(k+1\,|\,k),\ldots,y(k+\mathrm{HP}\,|\,k)\}^{\mathrm{T}}$ is the vector (dimension HPx1) of output predictions at instant k for instant $k+1$ to $k+\mathrm{HP}$; $\hat{\boldsymbol{z}}_a(k\,|\,k)$ is the state vector at instant k; $\Delta f_d(k) = f_d(k)$-$f_d(k$-1) is the force input move; $\boldsymbol{A}_g(k) = \boldsymbol{1}\cdot a_g(k)$ is the vector (dimension HPx1) of measured and future disturbances (in this case equal to the last measured value); and $\boldsymbol{\Psi}$, $\boldsymbol{\Theta}$ and $\boldsymbol{\Xi}$ are constant matrices derived from the system model – Eq. (15).

The optimal input force moves $\Delta f_d(k)$ can be obtained as the solution of an unconstrained optimization problem (minimization) with the cost function in Eq. (16).

$$\begin{aligned}\boldsymbol{\Psi} &= \mathcal{C}_a\cdot\mathcal{A} \\ \boldsymbol{\Theta} &= \mathcal{C}_a\cdot\mathcal{B} \\ \boldsymbol{\Xi} &= \mathcal{C}_a\cdot\mathcal{E}\end{aligned}$$

with:

$$\mathcal{A} = \left[\left(\boldsymbol{A}_a\right)^{\mathrm{T}} \quad \ldots \quad \left(\boldsymbol{A}_a^{\mathrm{HP}}\right)^{\mathrm{T}}\right]^{\mathrm{T}}$$

$$\mathcal{B} = \left[\left(\boldsymbol{B}_a\right)^{\mathrm{T}} \quad \ldots \quad \left(\sum_{j=0}^{j=\mathrm{HP}-1}\boldsymbol{A}_a^{\,j}\cdot\boldsymbol{B}_a\right)^{\mathrm{T}}\right]^{\mathrm{T}}$$

$$\mathcal{E} = \begin{bmatrix} \boldsymbol{E}_a & \boldsymbol{0} & \ldots & \boldsymbol{0} \\ \boldsymbol{A}_a\cdot\boldsymbol{E}_a & \boldsymbol{E}_a & \cdots & \boldsymbol{0} \\ \vdots & \vdots & \ddots & \vdots \\ \boldsymbol{A}_a^{\mathrm{HP-1}}\cdot\boldsymbol{E}_a & \boldsymbol{A}_a^{\mathrm{HP-2}}\cdot\boldsymbol{E}_a & \cdots & \boldsymbol{E}_a \end{bmatrix}$$

$$\mathcal{C}_a = \mathrm{diag}\left(\boldsymbol{C}_a \quad \ldots \quad \boldsymbol{C}_a\right) \tag{15}$$

$$\begin{aligned}V(k) &= \sum_{i=1}^{\mathrm{HP}}\left\|\hat{y}(k+i\,|\,k)\right\|_q^2 + \left\|\Delta f_d(k)\right\|_r^2 \\ &= \left\|\boldsymbol{Y}(k)\right\|_{\mathcal{Q}}^2 + \left\|\Delta f_d(k)\right\|_r^2\end{aligned} \tag{16}$$

where: q and r are the weighting values on the output and input moves respectively; $\mathcal{Q} = \mathrm{diag}(q \ \ldots \ q)$ is a weighting matrix (dimension HPxHP). The solution of this optimization problem is obtained by finding the gradient of the cost function and set it to zero:

$$\begin{aligned}\Delta f_d(k) &= \frac{1}{2}\mathcal{H}_t^{-1}\cdot\mathcal{G}_t \\ &= \boldsymbol{C}_1\cdot\hat{\boldsymbol{z}}_a(k\,|\,k) + \boldsymbol{C}_2\cdot f_d(k-1) + \boldsymbol{C}_3\cdot a_g(k)\end{aligned} \tag{17}$$

with: $\mathcal{H}_t = \boldsymbol{\Theta}^{\mathrm{T}}\cdot\mathcal{Q}\cdot\boldsymbol{\Theta} + r$; $\mathcal{G}_t = 2\cdot\boldsymbol{\Theta}^{\mathrm{T}}\cdot\mathcal{Q}\cdot\boldsymbol{E}(k)$; $\boldsymbol{E}(k) = -\boldsymbol{\Psi}\cdot\hat{\boldsymbol{z}}_a(k\,|\,k) - \boldsymbol{\Theta}\cdot f_d(k-1) - \boldsymbol{\Xi}\cdot\boldsymbol{A}_g(k)$ is the tracking error (difference between the future target, which is zero, and the free response, $\Delta f_d(k) = 0$); $\boldsymbol{C}_1 = -\boldsymbol{T}_t\cdot\boldsymbol{\Psi}$; $\boldsymbol{C}_2 = -\boldsymbol{T}_t\cdot\boldsymbol{\Theta}$; $\boldsymbol{C}_3 = -\boldsymbol{T}_t\cdot\boldsymbol{\Xi}\cdot\boldsymbol{1}$; and $\boldsymbol{T}_t = \mathcal{H}_t^{-1}\cdot\boldsymbol{\Theta}^{\mathrm{T}}\cdot\mathcal{Q}$. In order to guarantee the minimum solution the second derivative, or the Hessian matrix of $V(k)$, should be positive definite. This condition is verified if at least one weighting value is positive and the other is greater or equal to zero. Moreover, the closed-loop system (linear counterpart, considering $f = f_d$) should be stable when designing the MPC controller. Substituting Eq. (17) in Eq. (13), the closed loop system is found:

$$\begin{aligned}\boldsymbol{z}_a(k+1) = \left[\boldsymbol{A}_a + \boldsymbol{B}_a\cdot\boldsymbol{C}_1 + \boldsymbol{B}_a\cdot(\boldsymbol{C}_2+1)\cdot\boldsymbol{M}_{01}\right]\cdot\boldsymbol{z}_a(k) \\ + \left[\boldsymbol{E}_a + \boldsymbol{B}_a\cdot\boldsymbol{C}_3\right]\cdot a_g(k)\end{aligned} \tag{18}$$

where: $\boldsymbol{M}_{01}$ is the matrix that satisfies $f_d(k\text{-}1) = \boldsymbol{M}_{01}\cdot\boldsymbol{z}_a(k)$. Thus, q and r should be chosen such that the dynamic matrix eigenvalues of Eq. (18) lie in the unit circle.

The predictive controller described has several adjustable parameters: weights (acceleration weight q and input move weight r), prediction horizon HP and the control interval T_s. The results of a preliminary analysis showed that a control interval $T_s = 5$ ms is adequate for the problem under study. Moreover, a prediction horizon HP = 50 was chosen since the internal model has input delays $d = 10$ (50 ms) to account for the device time response. A unitary value for the input move weight was considered ($r = 1$ m/N) and the output weight q was tuned through numerical simulations considering a representative sample of input ground motions (accelerograms) under the range of stable solutions in order to identify the lowest mean peak acceleration.

4.1.4 Variable damping algorithm

This algorithm uses the inverse mathematical model of the device to compute the control variable:

$$c_v = \frac{T_d\cdot\dot{f}_d + f_d}{\dot{x}_r},\ c_{\min} \le c_v \le c_{\max} \tag{19}$$

The desired force f_d, its derivative (which is numerically computed) and the relative velocity $\dot{x}_{0g}$ are needed to compute the damping value. The relative velocity is considered a small constant $\varepsilon = 10^{-4}$ m/s when $\dot{x}_{0g} \le \varepsilon$ to avoid division by zero.

4.1.5 Clipped on-off algorithm

A different algorithm (bang-bang type) for computing the control variable is based on the two-position or on-off control action (Ogata, 1970) where the control law

is dependent on the actuating error signal (difference between the desired and the device force). The idea is that the maximum value should only be applied if the device force modulus is less than the desired force modulus and both have the same sign, which is given by the following equation:

$$c_{\mathrm{v}} = c_{\min} + (c_{\max} - c_{\min}) \cdot \mathrm{H}[(f_{\mathrm{d}} - f) \cdot f] \qquad (20)$$

where H[·] is the Heaviside step function.

4.2 Nonlinear output feedback control

A nonlinear output feedback control strategy (NOFC) is considered to derive the control law (Fig. 3). This approach involves a transformation of a nonlinear system into a linear and controllable one by a suitable nonlinear feedback law, which can then be tackled using linear control strategies (Isidori, 1995).

The procedure to derive the control law involves the whole system (structure and device) formulation described in Eq. (4).

Taking $f(\boldsymbol{z}_{\mathrm{c}}) = \boldsymbol{A}_{\mathrm{c}} \cdot \boldsymbol{z}_{\mathrm{c}}$, $h(\boldsymbol{z}_{\mathrm{c}}) = [-k_{\mathrm{b}}/m, -c_{\mathrm{b}}/m, -1/m] \cdot \boldsymbol{z}_{\mathrm{c}}$ and assuming that disturbance (earthquake) $\ddot{x}_{\mathrm{g}}$ is available for measurement then a control law can be established as (Isidori, 1995):

$$u(\boldsymbol{z}_{\boldsymbol{c}}) = a(\boldsymbol{z}_{\boldsymbol{c}}) + b(\boldsymbol{z}_{\boldsymbol{c}}) \cdot v + c(\boldsymbol{z}_{\boldsymbol{c}}) \cdot \ddot{x}_{\mathrm{g}} \qquad (21)$$

$a(\boldsymbol{z}_{\mathrm{c}})$, $b(\boldsymbol{z}_{\mathrm{c}})$ and $c(\boldsymbol{z}_{\mathrm{c}})$ result from the time derivative r of the output $\boldsymbol{y}_{\mathrm{c}}$ that has the input explicitly dependent, which is set equal to a reference v. Solving it in order to $u(\boldsymbol{z}_{\mathrm{c}})$, one finds: $a(\boldsymbol{z}_{\mathrm{c}}) = -b(\boldsymbol{z}_{\mathrm{c}}) \cdot \mathrm{L}_f^r h(\boldsymbol{z}_{\mathrm{c}})$, $b(\boldsymbol{z}_{\mathrm{c}}) = 1 / \mathrm{L}_g \mathrm{L}_f^{r-1} h(\boldsymbol{z}_{\mathrm{c}})$, $c(\boldsymbol{z}_{\mathrm{c}}) = -b(\boldsymbol{z}_{\mathrm{c}}) \cdot \mathrm{L}_p \mathrm{L}_f^{r-1} h(\boldsymbol{z}_{\mathrm{c}})$, $\mathrm{L}_f^k h(\boldsymbol{z}_{\mathrm{c}}) = \nabla^k h(\boldsymbol{z}_{\mathrm{c}}) \cdot f(\boldsymbol{z}_{\mathrm{c}})$ as the k derivative of $h(\boldsymbol{z}_{\mathrm{c}})$ along $f(\boldsymbol{z}_{\mathrm{c}})$, ($k$ Lie derivative). The number of time derivatives evaluated to find that relationship is called relative degree (denoted as r). For the problem described by the system in Eq. (4), the relative degree is $r = 1$ if $\mathrm{L}_g \mathrm{L}_f^{r-1} h(\boldsymbol{z}_{\mathrm{c}}) \neq 0$. In order to accomplish this requirement the input vector is modified. The input vector $g(\boldsymbol{z}_{\mathrm{c}})$ is modified by adding a small constant to the last entry, without modifying considerably the solution:

$$g(\boldsymbol{z}_{\mathrm{c}}) = \\ = \left[0 \quad 0 \quad \dot{x}_{0\mathrm{g}} / T_{\mathrm{d}} + \varepsilon_{\mathrm{a}} \cdot \mathrm{sgn}(\dot{x}_{0\mathrm{g}} / T_{\mathrm{d}} + \varepsilon_{\mathrm{a}})\right]^{\mathrm{T}} \qquad (22)$$

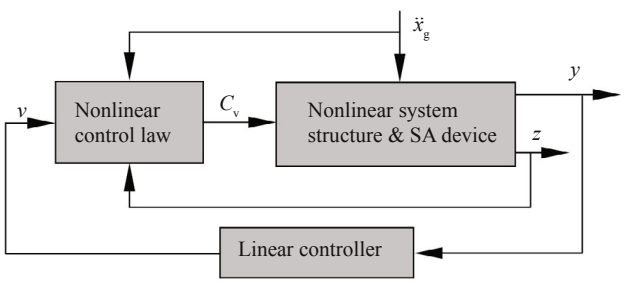

Fig. 3 Nonlinear output feedback control strategy

For the problem under study $\varepsilon_{\mathrm{a}} = 10^{-4}$ m/s^2 was considered adequate. The terms for the control law in Eq. (21) are then given by:

$$a(\boldsymbol{z}_{\mathrm{c}}) = \frac{k_{\mathrm{b}} \cdot c_{\mathrm{b}}}{m} \frac{x_{0\mathrm{g}}}{D} + \\ \left(\frac{c_{\mathrm{b}}^2}{m} - k_{\mathrm{b}}\right) \frac{\dot{x}_{0\mathrm{g}}}{D} + \left(\frac{c_{\mathrm{b}}}{m} + \frac{1}{T_{\mathrm{d}}}\right) \frac{f}{D}$$

$$b(\boldsymbol{z}_{\mathrm{c}}) = -\frac{m}{D}$$

$$c(\boldsymbol{z}_{\mathrm{c}}) = \frac{c_{\mathrm{b}}}{D}, \quad D = \frac{\dot{x}_{0\mathrm{g}}}{T_{\mathrm{d}}} + \varepsilon_{\mathrm{a}} \cdot \mathrm{sgn}\left(\frac{\dot{x}_{0\mathrm{g}}}{T_{\mathrm{d}}} + \varepsilon_{\mathrm{a}}\right) \qquad (23)$$

Reference v in Eq. (21) is the output of a linear controller having as input the tracking error, which for the present problem (regulation) is a negative feedback from the base floor acceleration $\boldsymbol{y} = \ddot{x}_0$. A linear and controllable system will be obtained between the output and the reference v that can be tackled by a suitable control law:

$$y^r = v \Leftrightarrow \dot{y} = v \\ v = -\sum_{j=0}^{r-1} k_j \cdot y^j \Leftrightarrow v = -k_0 \cdot \ddot{x}_0 \qquad (24)$$

whose parameters $k_j = k_0 > 0$ should be chosen so that the roots lie in the left half plane in order to achieve convergence to zero as time goes to infinity. In Eq. (21) the control variable $u(\boldsymbol{z}_{\mathrm{c}})$ was used instead of c_{v} because the input damping is bounded $c_{\min} \leq c_{\mathrm{v}} \leq c_{\max}$. Thus the following rule is considered to meet that restriction:

$$c_{\mathrm{v}} = \begin{cases} c_{\min}, & u(\boldsymbol{z}_{\mathrm{c}}) < c_{\min} \\ u(\boldsymbol{z}_{\mathrm{c}}), & c_{\min} \leq u(\boldsymbol{z}_{\mathrm{c}}) \leq c_{\max} \\ c_{\max}, & u(\boldsymbol{z}_{\mathrm{c}}) > c_{\max} \end{cases} \qquad (25)$$

The derived control law should keep the variables that represent the system internal behaviour bounded. From Eq. (25) it is stated that the input damping for the system is bounded $c_{\min} \leq c_{\mathrm{v}} \leq c_{\max}$ and thus the input damping just modifies the dissipative force and has not authority to destabilize the system. The resulting closed-loop system is then always asymptotic stable.

The implementation of this control strategy requires also the definition of the linear controller gain k_0. The controller gain was tuned as in the previous cases, through numerical simulations considering a representative sample of input ground motions (accelerograms) of the site were the structure is to be installed and select the gain (or damping) that minimizes the mean peak acceleration responses.

5 Numerical simulations

In this section structural models subjected to typical Portuguese seismic actions will be used to verify the effectiveness of the proposed control strategies for controlling the SA devices. Two different types of input ground motions for near and far-field are considered in the simulations. Concerning to the structural models, a SDOF mechanical model will be considered first to evaluate the applicability of these strategies to base-isolated buildings. In the end a numerical example of a typical 10-storey base-isolated building model (multi degree of freedom model - MDOF) is considered to evaluate the performance of the proposed control strategies. Comparisons are made with the original structure (structural model only) and with the structure equipped with optimized passive devices (with fixed damping value) at the isolation level, referred as the passive system. Passive devices are described by the following law $f_p = c_p \cdot |\dot{x}_r|^{\alpha} \cdot \mathrm{sgn}(\dot{x}_r)$ with: f_p as the force provided by the damper; c_p is the damping coefficient; $\dot{x}_r = \dot{x}_{0g}$ is the relative velocity between the cylinder case and the piston head of the damper; and α is the velocity exponent. α = 0.15 is considered for the SDOF model and α = 1 for the MDOF model, since those values lead to the best passive system performance.

5.1 Earthquake ground motions

The input actions used in this work are representative of the two different types of ground motions for the Portuguese territory: near and far field (Figs. 4(a)-(b)).

Artificial accelerograms were generated using the response spectrums provided in the Eurocode 8 for Portugal (NP EN 1998-1, 2010) for Type 1 (far field) seismic action and Type 2 (near field) seismic action. Ten accelerograms were generated for each type of seismic action. The accelerograms are representative of zone 1, soil type D, for structures of class II importance and for description of horizontal components of the seismic action. An example of typical accelerograms and their respective spectrums are depicted in Fig. 4. It is found that the generated accelerograms match the Eurocode National Annex response spectrums. It can be seen also that Type 1 accelerogrms have a longer duration and are richer in the lower frequencies (or higher periods) than Type 2 accelerograms.

5.2 Evaluation criteria

In order to analyse the performance of the structural systems under study, the time responses in terms of relative displacements, absolute accelerations, device force and base shear force resulting from each accelerogram as input were used to extract the peak values. Using the peak values from the 10 responses, the mean values are evaluated and used as a suitably representative value of the system response for each type of seismic action. The systems being analysed are the original structure (structural model only), the structure equipped with optimized passive devices (with fixed damping value) and the structure employing the SA devices under study. The performance of the proposed systems is evaluated in terms of ratios of those parameters in relation to the original structure ones. Good performance is thus associated with smaller ratios that should be less than one. Table 1 resumes the structural responses evaluation criteria considered in this work.

5.3 SDOF model analysis

5.3.1 SDOF system description

In base isolation systems the first mode of vibration contributes the most to the total response of the structure. This mode corresponds mainly to the deformation of the base isolation system. A SDOF mechanical model was first considered to model this behaviour, thus assuming a flexible base isolation system and a rigid superstructure.

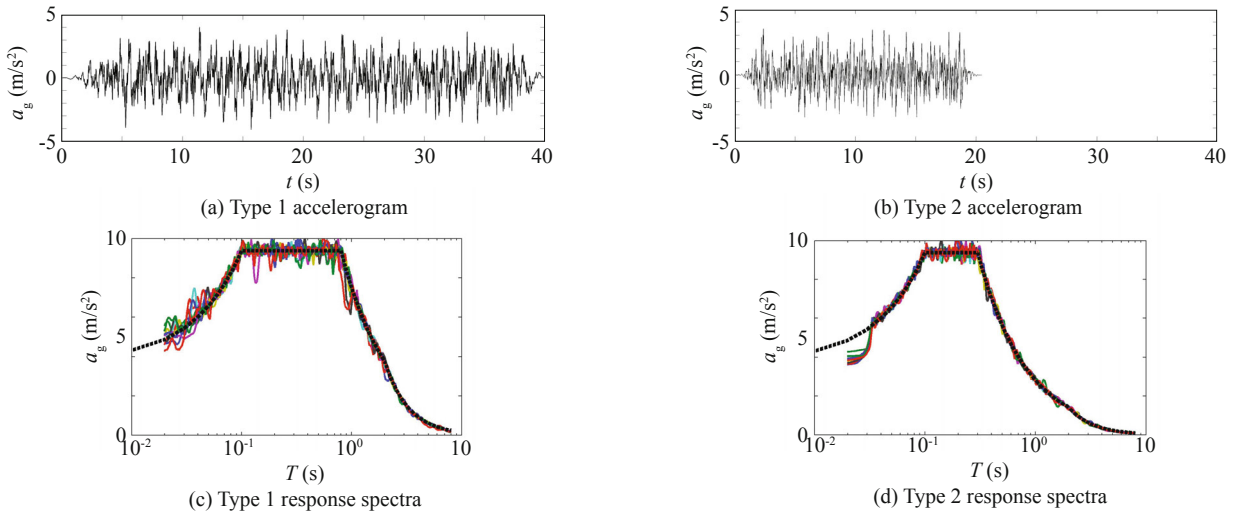

Fig. 4 Seismic actions: (a) & (b) example of one accelerogram for each seismic action type; (c) & (d) response spectra of the 10 accelerograms generated with Eurocode eleastic response spectra (in dash)

Table 1 Structural responses evaluation criteria

Parameter	Description
x	Specific time response x: x_{0g} – relative displacement of the base floor to the ground; x_{10g} – relative displacement of the top floor to the ground; a_0 – absolute acceleration at the base floor; a_{10} – absolute acceleration at the top floor; f – device force; V – base shear force;
P_x	Peak responses of x for one accelerogram;
M_x	Mean of peak responses of x from 10 accelerograms of the same type;
R_x	Ratio of mean of peak responses of x for a specific solution, passive or semi-active, relative to the mean of peak response of x for the original structure, from the 10 accelerograms of the same type;

In fact this was the approach considered previously in the control law formulations. Common base isolation systems are designed to have natural frequencies bellow 1 Hz. In order to evaluate the performance of several base isolation systems the following properties were considered: $m = 5750$ kg (mass), $f_b = 0.25$ to 1 Hz (natural frequency) and $\xi_b = 0.1$ (damping ratio).

5.3.2 SDOF original structure and passive system

The results of the original structure for different natural frequencies subjected to Type 1 and 2 seismic actions are shown in Table 2.

Concerning to the structural system with optimized passive devices, the parameters of the model should be defined (damping coefficient c_p and velocity exponent α). A preliminary analysis showed that the lower velocity exponents always lead to better performance. Recent technological developments made available devices with velocity exponents $\alpha = 0.15$ (Castellano *et al.*, 2004), which is the value considered in this study for the SDOF model. The damping coefficient was chosen for each structural system taking into account the seismicity of the site using the set of generated accelerograms through numerical simulations. Typical evolution of system peak responses with the damping coefficient is found in Fig. 5. The results show that increasing the damping coefficient reduces the peak relative displacements but increases the peak accelerations. In order to reduce the relative displacements with small impact on the absolute accelerations, the minimum of mean peak accelerations (minimum of black dash curve in Fig. 5) was chosen as a criterion to define the damping constant c_p.

The correspondent values of the damping for the different natural frequencies and for both types of seismic action can be observed in Fig. 6. An increasing tendency of the damping as the system natural frequency increases can be detected. It is also clear that the selected damping values differ from distinct seismic actions, meaning that different damping values are needed to cope with different type of inputs.

The correspondent responses for those values of damping in terms of ratios relative to the original structure can be found in Table 3.

5.3.3 SDOF semi-active control

Semi-active devices defined according to Eq. (3) are dependent of the time constant T_d and of the variable damping coefficient c_v which is bounded between a minimum c_{min} and maximum c_{max} values. The type of device and the available solution determine the values of those parameters, which by themselves have influence on the whole system performance. In previous works

Table 2 SDOF original structure mean peak responses

f_b (Hz)	0.25	0.37	0.50	0.62	0.75	0.87	1.00
			Type 1 seismic action				
Mx_{0g} (m)	0.293	0.278	0.266	0.222	0.187	0.155	0.131
Ma_0 (m/s^2)	0.765	1.554	2.694	3.457	4.253	4.742	5.298
			Type 2 seismic action				
Mx_{0g} (m)	0.113	0.109	0.104	0.0845	0.0704	0.0602	0.0516
Ma_0 (m/s^2)	0.300	0.623	1.062	1.320	1.618	1.848	2.088

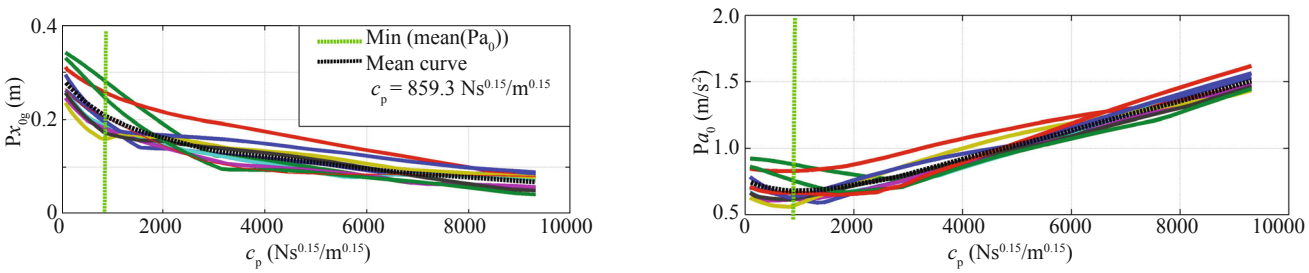

Fig. 5 Peak responses of the SDOF model (f_b = 0.25 Hz; ξ_b = 0.1) with a passive damper vs. device damping when subjected to 10 input Type 1 accelerograms

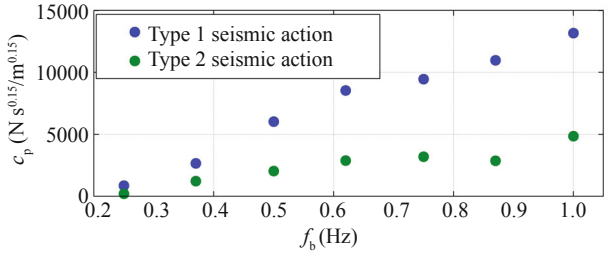

Fig. 6 Damping coefficients for the minimum mean of peak acceleration response vs. SDOF system natural frequencies

several values have been considered for the range of damping in which the device can be changed [c_{min}, c_{max}]. Sadek and Mohraz (1998) considered a range defined by the damping ratio of the structure first mode of vibration between 5% and 40%. Gavin and Aldemir (2005) referred damping ratio ranges between 6% and 54% or even between 9% and 87%. Other authors referred values that can manipulate the first mode damping ratio between 5% and 16%, approximately (Symans and Constantinou, 1995; Komatsu *et al.*, 2007). In this work a range of damping between 5% and 45% of the critical damping is considered based in the results of a preliminary study where it was found that higher damping values for c_{max} do not provide relevant performance improvements. Concerning to the time constant, previous experimental works referred time constants around T_d = 50 ms for the SA fluid dampers (Symans and Constantinou, 1995; Komatsu *et al.*, 2007) and around T_d = 6 ms for MR devices (Dyke and Spencer, 1997). A time constant T_d = 50 ms was considered in this work.

Recalling that in the formulation of the control laws, the controller parameters have to be defined to implement SA systems. In order to find the best controller parameters the seismicity of the site using a set of generated accelerograms is used to simulate the models for different controller parameters and identify the best value. As for the definition of the damping coefficient in passive devices, the minimum acceleration is the criterion considered in choosing the controller gain.

Concerning to integral control law with the associated algorithms (force tracking schemes I VD and I COO), the peak responses for each controller gain considering each input accelerogram were determined and the mean value was evaluated. An example of a typical evolution of the peak responses of the 10 input accelerograms with the controller gain is shown in Fig. 7.

It is found that the minimum of peak accelerations (and the mean value) are next to each other and around the same value of gain. The relative displacements are also reduced when compared to the values for smaller gains. The minimum of the mean peak responses is then chosen as the criterion to identify the controller gain. This procedure was considered in identifying the controller gain for other system natural frequencies. The correspondent system damping ratios ξ are calculated and the results obtained with different algorithms and type of seismic actions is depicted in Fig. 8.

Similar values are found independent of the seismic action and algorithm. The damping ratios lie between 40 and 90% approximately and have a decreasing tendency with the natural frequency. Although different values of damping ratio are found for the same system natural frequencies (different algorithms and input action type), small impact on the system response is observed if any value in that range is considered for the controller design. The correspondent responses provided by the force tracking schemes using the identified gains can be found in Table 3.

With the linear quadratic regulator controller two force tracking schemes (LQR VD and LQR COO) were also considered and the same procedure described previously was also used to identify the output weight q to design the controller gain vector $\boldsymbol{K}_y$. Figure 9 depicts the results of the output weight for different system natural frequencies and control algorithms.

As for the damping ratio in the integral control law, different output weighting values are found for the same system natural frequencies. Notice that higher weighting values are obtained for type 2 seismic actions and for VD algorithms, but small impact on the system response is observed if any value in that range is considered for the controller design. Responses provided by this force tracking schemes using the identified output weights can be found in Table 3.

The force tracking schemes using the model predictive controller (MPC VD and MPC COO) were

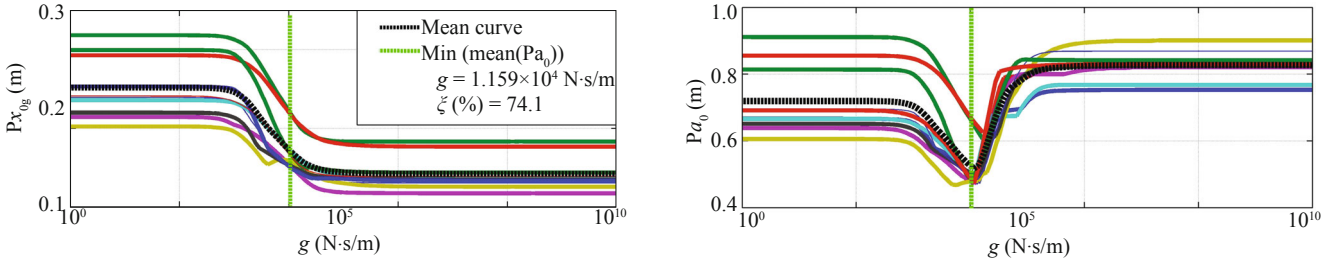

Fig. 7 Peak responses of the SDOF model (f_b = 0.25 Hz; ξ_b = 0.1) with an SA device plus I VD vs. controller gain when subjected to 10 input Type 1 accelerograms

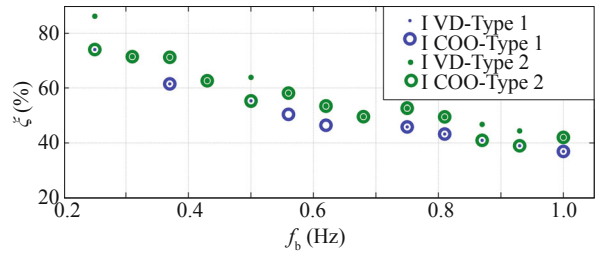

Fig. 8 SDOF system closed loop damping ratios (integral controller) function of its natural frequency

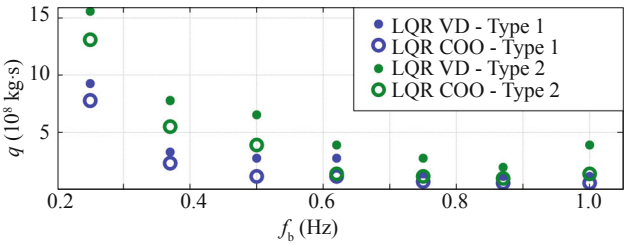

Fig. 9 LQR controller output weighs function of SDOF system natural frequency

also implemented to control the SA device. The output weight was identified in the same way to synthesize the MPC controller and the values are presented in Fig. 10.

Contrary to the LQR controller, the MPC output weight has an increasing tendency with the system natural frequency. These output weights are less sensitive to the seismic action type and control algorithm for the same system natural frequency. The responses provided by these tracking schemes with the identified output weights can be found in Table 3.

Finally the nonlinear output feedback control strategy (NOFC) was also implemented to control the SA device. Within this strategy the linear controller gain k_0 has to be identified. As for the previous cases numerical simulations were performed to analyse the influence of the controller gain on the peak responses. An example of a typical evolution of the peak responses for 10 input accelerograms is shown in Fig. 11.

It is found that higher gains always conduct to smaller responses that are insensitive to the gain value. Taking into account all the different system natural frequencies and type of seismic actions a controller gain $k_0 = 1000$ s^{-1} was chosen. The responses (peak values) provided by this strategy using the identified linear controller gains can be found in Table 3.

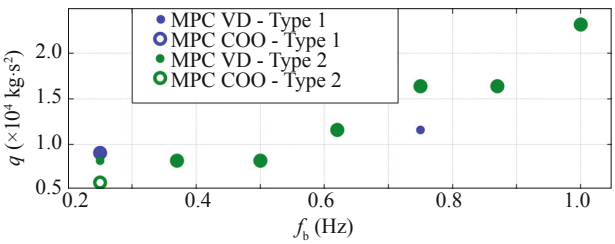

Fig. 10 MPC controller output weights function of SDOF system natural frequency

5.3.4 SDOF system: comparison of results

Having found the best parameters for the strategies under study, the mean peak responses for each structural system were determined. Table 3 shows the relative displacements and accelerations (mean peak values) in terms of ratios relative to the original structure responses for comparison. Ratios less than 1 indicate that the response of the structure with the added dissipation devices is lower than that of the original structure. It is found that any solution performs better than the original structure. Moreover, values in bold are identified as the ones with lower ratios than the passive solution. Thus, in terms of accelerations all force tracking schemes (I VD, I COO, LQR VD, LQR COO, MPC VD and MPC COO) perform better than the passive case for structural systems with natural frequencies bellow 0.6 Hz for Type 1 seismic actions, and below 1 Hz for Type 2 seismic actions (approximately), which is in the operational range of base-isolated structures. Base isolation systems should then employ semi-active devices driven by those force tracking schemes in such circumstances. Moreover, for lower natural frequency systems better performances than the passive case are also achieved in terms of relative displacements. It can also be seen that the SA device controlled by an on-off algorithm (COO) has a similar performance to the variable damping algorithm (VD). The nonlinear control strategy (NOFC), although easily tuned by choosing a higher gain value, does not perform as well as the

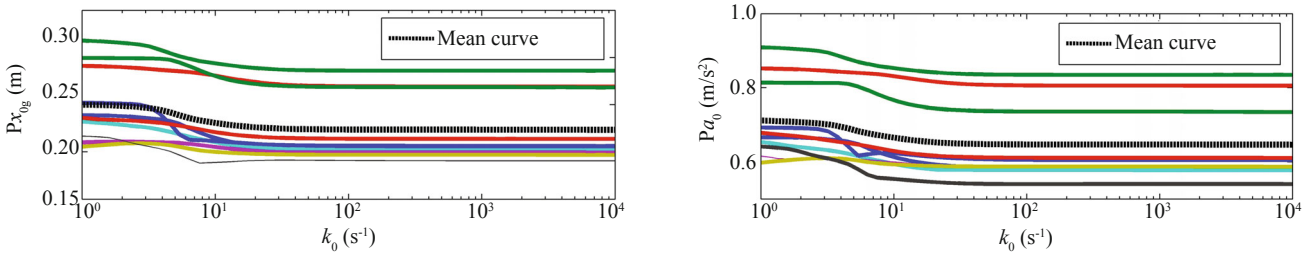

Fig. 11 Peak responses of the SDOF model ($f_b = 0.25$ Hz; $\xi_b = 0.1$) with an SA device plus NOFC vs. controller gain when subjected to 10 input Type 1 accelerograms

Table 3 Ratios of mean of peak responses for the SDOF structure with additional systems

f_b (Hz)	0.25	0.37	0.50	0.62	0.75	0.87	1.00	0.25	0.37	0.50	0.62	0.75	0.87	1.00
Type 1 seismic action														
	Rx_{0g}							Ra_0						
Passive	0.71	0.49	0.30	0.23	0.23	0.21	0.18	0.89	0.74	0.61	0.56	0.52	0.51	0.49
I VD	**0.58**	0.54	0.48	0.48	0.49	0.51	0.51	**0.68**	**0.60**	**0.53**	**0.55**	0.56	0.57	0.57
I COO	**0.58**	0.54	0.48	0.50	0.50	0.52	0.52	**0.68**	**0.60**	**0.53**	**0.54**	0.56	0.57	0.56
LQR VD	**0.62**	0.56	0.50	0.51	0.52	0.54	0.54	**0.72**	**0.62**	**0.55**	**0.56**	0.56	0.58	0.58
LQR COO	**0.64**	0.56	0.50	0.51	0.54	0.56	0.56	**0.73**	**0.62**	**0.55**	**0.56**	0.57	0.59	0.59
MPC VD	**0.57**	0.54	0.50	0.51	0.54	0.53	0.50	**0.69**	**0.61**	**0.55**	0.57	0.58	0.59	0.58
MPC COO	**0.58**	0.54	0.51	0.52	0.51	0.56	0.53	**0.71**	**0.63**	**0.56**	0.58	0.59	0.60	0.58
NOFC	0.76	0.69	0.67	0.69	0.70	0.71	0.70	**0.85**	**0.74**	0.71	0.73	0.73	0.74	0.73
Type 2 seismic action														
	Rx_{0g}							Ra_0						
Passive	0.86	0.55	0.44	0.42	0.43	0.49	0.41	0.97	0.81	0.69	0.70	0.67	0.68	0.70
I VD	**0.59**	**0.53**	0.48	0.53	0.55	0.57	0.59	**0.73**	**0.62**	**0.58**	**0.63**	**0.62**	**0.64**	**0.68**
I COO	**0.60**	**0.54**	0.50	0.54	0.55	0.58	0.58	**0.74**	**0.63**	**0.57**	**0.61**	**0.61**	**0.63**	**0.65**
LQR VD	**0.64**	0.59	0.55	0.57	0.59	0.58	0.59	**0.77**	**0.66**	**0.60**	**0.64**	**0.65**	**0.65**	**0.66**
LQR COO	**0.65**	0.60	0.55	0.57	0.59	0.59	0.59	**0.79**	**0.67**	**0.60**	**0.65**	**0.65**	**0.64**	**0.65**
MPC VD	**0.58**	0.55	0.51	0.55	0.55	0.59	0.60	**0.75**	**0.65**	**0.58**	**0.64**	**0.64**	**0.65**	**0.68**
MPC COO	**0.62**	0.57	0.53	0.56	0.57	0.60	0.61	**0.78**	**0.67**	**0.60**	**0.65**	**0.63**	**0.66**	**0.68**
NOFC	**0.78**	0.73	0.68	0.74	0.74	0.73	0.71	**0.90**	**0.79**	0.73	0.79	0.78	0.78	0.76

force tracking schemes. The results also show that the force tracking schemes using an integral control law provide the best results. Those SA systems (I VD and I COO) can provide reductions in relative displacements (between 50 % to 60 % approximately) when compared to the original structure and improve the acceleration responses when compared with the passive case on the same circumstances ($f_b \leq 0.6$ Hz for Type 1 seismic actions and $f_b \leq 1$ Hz for Type 2 seismic actions). An example comparing the time responses and the inputs (damping coefficient and force) of the original system, passive and SA system, for one input accelerogram is presented in Fig. 12. It is shown that changing damping in real time with a well tuned controller improves the system performance (in terms of relative displacements and absolute accelerations).

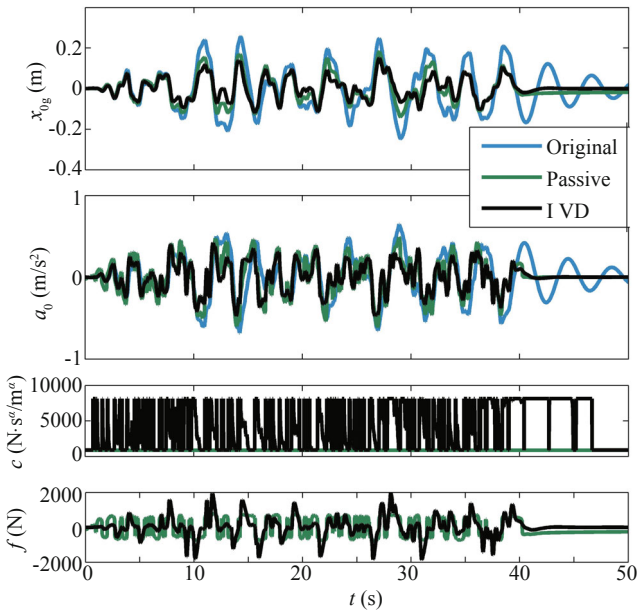

Fig. 12 Time histories of rel. displacement, accel., input damping and force for the SDOF model (f_b = 0.25 Hz; ξ_b = 0.1) subjected to one Type 1 accelerogram

5.4 MDOF model analysis

5.4.1 MDOF structural system

A 10-storey base-isolated structure represented by a unidirectional lumped-mass system (Fig. 13(a)) representative of a 10-storey dual frame-wall structure was used to evaluate the effectiveness of the proposed strategies. The superstructure fundamental frequency is f_{sf} = 1.6 Hz and the damping ratio is ξ_{sf} = 5 %. Each floor has a constant mass described by $m_f = 10^5$ kg. The stiffness and damping matrices were obtained considering constant stiffness between floors and a stiffness proportional damping matrix ($\boldsymbol{C} = a_0 \cdot \boldsymbol{K}$), which correspond to stiffness and damping coefficients between floors of k_f = 452.43 kN/mm and c_f = 1.51 kN·s/mm with a_0 = 0.0033 s. The superstructure is supported on a base isolation system with a mass of $m_b = 1.4 \cdot m_f$ and laminated natural rubber bearings represented by a

linear elastic and viscous model, with a target frequency $f_b = 0.4$ Hz and an equivalent damping ratio of $\xi_b = 10$ %. The correspondent stiffness and damping coefficients were obtained assuming a rigid superstructure with a total mass of $m = 11.4 \cdot m_f$, $k_b = 7.20$ kN/mm and $c_b = 0.57$ kN·s/mm. The base isolation system model is assembled to the superstructure model and the resultant base-isolated structure modal frequencies and damping ratios (first three) are: $f_1 = 0.39$ Hz, $\xi_1 = 9.34$ %; $f_2 = 2.99$ Hz, $\xi_2 = 5.57$ %; and $f_3 = 5.87$ Hz, $\xi_3 = 7.23$ %.

Additional devices are installed at the base level connecting the ground to the base isolation system mass (base floor mass).

Apart from the original structure, two passive systems (with constant damping and velocity exponent $\alpha = 1$) were considered for comparison with the SA systems: Passive C_{id} with the device having a damping coefficient $c_{id} = 1.1$ kN·s/mm (additional damping of $\xi_{id} = 0.19$), which is the damping that leads the structure to a relative displacement similar to the structure employing an SA system; and Passive C_{max} with the device having the maximum damping considered for the SA device, $c_{max} = 2.58$ kN·s/mm (additional damping of $\xi_{max} = 0.45$).

SA devices with the same characteristics of those in previous examples were taken into account: time constant $T_d = 0.05$ s; and additional damping varying between $0.05 \le \xi_{ad} \le 0.45$ relative to the isolation critical damping, $c_c = 2 \cdot m \cdot \omega_b$, where $\omega_b = 2 \cdot \pi \cdot f_b$. Using the same procedure to tune the controllers as for the SDOF model, the following values were obtained for each control strategy: $g = 1.5$ kN·s/mm for I VD and I COO; $q = 5.1\text{x}10^{11}$ kg·s for LQR VD and $q = 2.5\text{x}10^{11}$ kg·s for LQR COO, both with $r = 1$ s/kg; $q = 10^8$ kg·s^2, $r = 1$ m/N, HP = 50, $T_s = 5$ ms $d = 10$ for MPC VD and MPC COO; and $k_0 = 1000$ s^{-1} for NOFC. Notice that different values are considered for the LQR controller. Different output weighting values were found for the algorithms considered and seismic action type. A compromise was assumed when using the same weight for different seismic actions type. It should be mentioned that better performance would be obtained if four weighting values were used (one for each combination of algorithm and seismic action).

5.4.2 MDOF system: comparison of results

The results obtained with each structural system for both seismic actions type in terms of mean peak responses for the relative displacements and accelerations along structure floor can be found in Figs. 13(b) & (c). The ratios of the mean peak responses and base shear force MV in relation to the original structure responses as well as the ratio of the mean peak device force in relation to the structure weight Mf/W are presented in Table 4. Values in bold are identified as the ones with lower ratios than the Passive C_{id} solution and underlined are those with ratios greater than one. All solutions reduce the structure relative displacements with the maximum damping passive case being the best one for this criterion. However, an increase in the acceleration responses is observed, namely for Type 2 seismic actions, where the highest amplifications are verified. It was found that SA strategies perform better than the optimized passive case in terms of accelerations and at the same time provide better reductions than the original structure in terms of relative displacements. However, the SA system with an optimal controller (LQR) subjected to type 2 seismic actions has inferior performance than the original structure. In fact this controller was tuned considering both seismic actions type and thus better results would be found if the controller was tuned for each seismic action separately.

The Passive C_{id} case which is the one having relative displacements similar to the I VD controller, shows inferior performance in terms of absolute accelerations when compared to the SA one, meaning that those SA solutions are always better in reducing the absolute accelerations. As for the SDOF systems the best SA

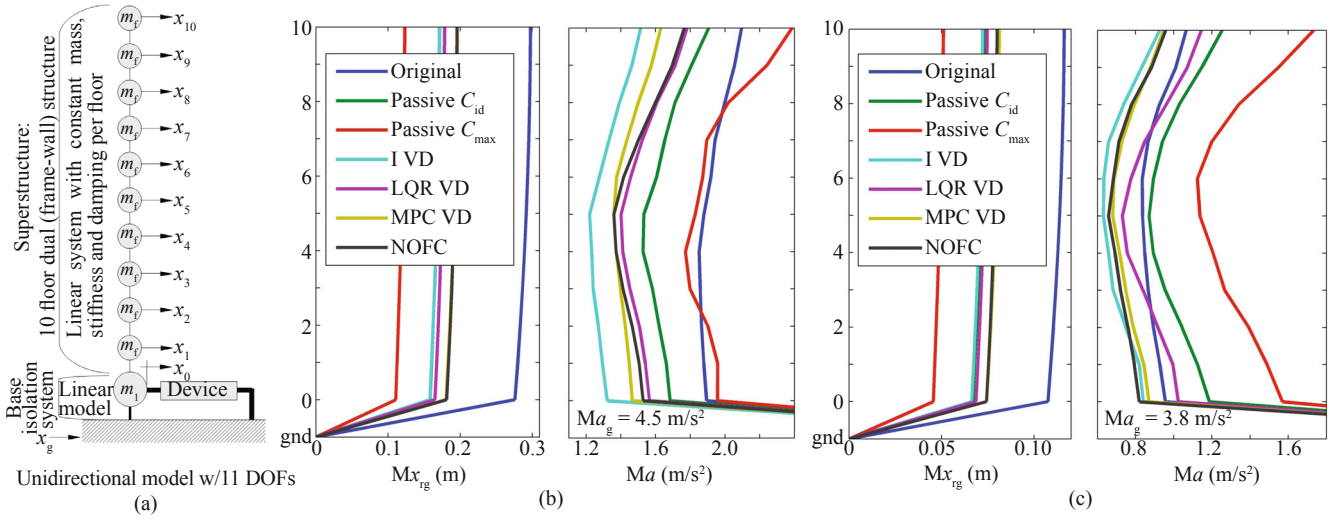

Fig. 13 MDOF structural model responses: (a) lumped-mass model; (b) responses to Type 1 seismic actions; (c) responses to Type 2 seismic actions

Table 4 MDOF system responses: comparisons with the original structure

Original	Type 1 seismic action						Type 2 seismic action					
	Mx_{0g} (m)	Mx_{10g} (m)	Ma_0 (m/s²)	Ma_{10} (m/s²)	MV (kN)	-	Mx_{0g} (m)	Mx_{10g} (m)	Ma_0 (m/s²)	Ma_{10} (m/s²)	MV (kN)	-
	0.276	0.298	1.894	2.095	2050	-	0.108	0.116	0.957	1.065	818	-
	Rx_{0g}	Rx_{10g}	Ra_0	Ra_{10}	RV	Mf/W	Rx_{0g}	Rx_{10g}	Ra_0	Ra_{10}	RV	Mf/W
Passive C_{id}	0.57	0.58	0.89	0.91	0.74	0.06	0.62	0.63	1.24	1.18	0.80	0.02
Passive C_{max}	**0.4**	**0.41**	1.03	1.14	0.78	0.10	**0.42**	**0.44**	1.64	1.63	0.93	0.05
I VD	**0.57**	**0.58**	**0.70**	**0.72**	**0.62**	**0.05**	**0.62**	**0.62**	**0.88**	**0.87**	**0.68**	**0.02**
I COO	0.58	**0.58**	**0.75**	**0.74**	**0.63**	**0.05**	**0.62**	**0.62**	**1.00**	**0.95**	**0.68**	**0.02**
LQR VD	0.60	0.60	**0.83**	**0.85**	**0.70**	**0.05**	0.64	0.64	**1.07**	**1.07**	**0.75**	**0.02**
LQR COO	0.67	0.67	**0.88**	**0.86**	**0.73**	**0.04**	0.70	0.71	**1.13**	**1.06**	**0.78**	**0.02**
MPC VD	0.65	0.66	**0.77**	**0.78**	**0.70**	**0.04**	0.69	0.70	**0.91**	**0.89**	**0.75**	**0.02**
MPC COO	0.66	0.66	**0.81**	**0.81**	**0.71**	**0.04**	0.69	0.70	**0.98**	**0.93**	**0.75**	**0.02**
NOFC	0.66	0.66	**0.81**	**0.84**	**0.70**	**0.09**	0.69	0.69	**0.86**	**0.90**	**0.75**	**0.03**

system is the I VD. More elaborate strategies, like NOFC or even the force tracking schemes using MPC controllers, do not perform better than those with I VD. It is verified also that force tracking schemes with variable damping algorithms (VD) usually provide better performance than those with clipped on-off algorithms (COO). SA systems also perform better than the passive ones in terms of base shear forces transmitted to the structure at the base, since part of the seismic force is dissipated by the devices. For the same reason, force tracking schemes with an integral controller provide better performance than the other strategies. It is shown that SA device control forces (mean peak values) are always below 10 % of the structure weight.

The control effectiveness of SA systems can be observed in Fig. 14 where the time response at the base, upper floor and the inputs (damping coefficient and force) with one input accelerogram for the original system, with Passive C_{id} and with I VD systems is shown.

The results obtained with the MDOF model also showed that changing damping in real time with an adequate control strategy can improve the structural system performance by reducing both relative displacements and absolute accelerations.

6 Conclusions

This work presents a comparative study of several control strategies to drive semi-active energy dissipation devices installed at the isolation level of base-isolated structures for earthquake response reduction.

Based on the results of the SDOF model the I VD showed to be the best SA control strategy in reducing both acceleration and relative displacement. The I COO and MPC strategies came in second providing overall good performance. I VD clearly outperformed the original structure and the structural system with optimized passive devices for natural frequencies bellow 0–6 Hz subjected to both type 1 and type 2 artificially generated accelerograms. The nonlinear output feedback

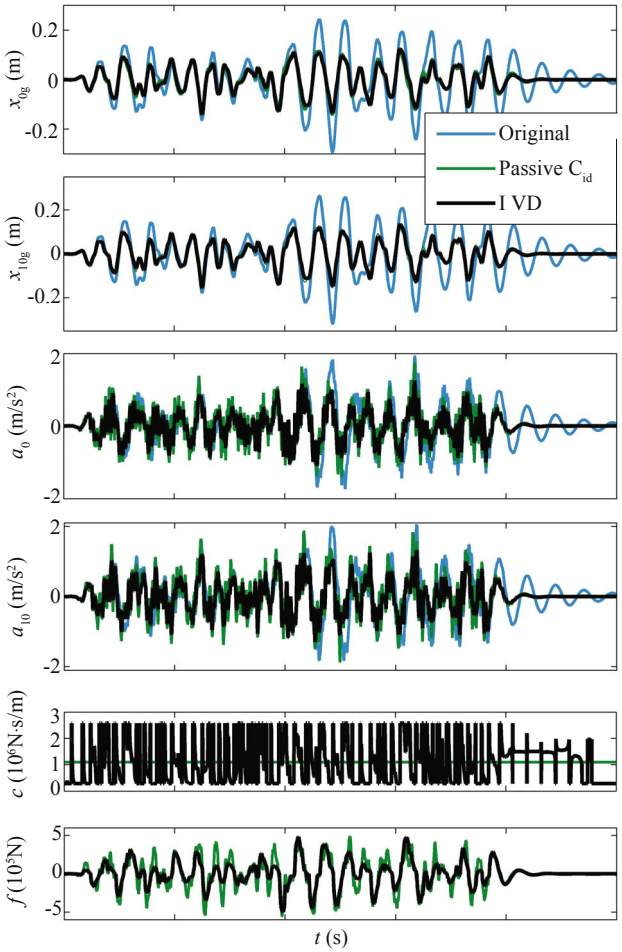

Fig. 14 Time histories of base and top floor relative displacements and accelerations, input damping and force for the MDOF model subjected to one Type 1 accelerogram

controller NOFC showed to be effective in terms of accelerations on the SDOF model only for lower natural frequency systems, but showed slightly higher relative displacements than the other SA solutions. The LQR controllers showed to be among the force tracking controllers the ones with inferior performance. The results also showed that VD and COO algorithms provided similar performance, with a slight performance advantage of the VD algorithm. For the MDOF system VD algorithms always performed better than COO algorithms. Moreover, with the MDOF model all strategies could reduce the relative displacements of the structure and at the same time improve the accelerations responses better than the optimized passive devices. As for the SDOF model the I VD control strategy showed to be the best SA control strategy and I COO the second best one for type 1 seismic action. For type 2 seismic actions MPC VD was the second best control strategy in terms of acceleration performance. The NOFC strategy is in general better than the LQR force tracking schemes in terms of accelerations but not in terms of relative displacements. It was found that the LQR force tracking schemes showed the lowest performance in terms of accelerations for type 2 seismic actions, resulting from the fact that this controller synthesis was highly dependent of the seismic action type and algorithm.

As a general conclusion, it was found possible to improve the behaviour of base-isolated structures with SA systems, with the I VD being the best strategy among those analysed here. With this solution the best compromise in reducing both relative displacements and accelerations was achieved. The other solutions were not as effective in this fashion. The passive case with maximum damping in particular was the best one in reducing the base floor relative displacements, but at the expense of increasing the accelerations and upper floor relative displacements. It was shown that the controller gain had a large influence in system performance and thus, its design should be thoroughly analysed. It is recommended to identify the controller gain using a model of the structure subjected to a set of representative ground motions of the site and select the value that minimizes the peak accelerations.

Acknowledgement

The authors would like to thank the Portuguese Foundation for Science and Technology (FCT) for the PhD scholarship provided (reference SFRH/BD/84769/2012) and, to the National Laboratory for Civil Engineering (LNEC) and Instituto Superior Técnico (IST) for providing the resources available to develop this work.

References

Aguirre N, Ikhouane F and Rodellar J (2011), "Proportional-plus-integral Semiactive Control Using Magnetorheological Dampers," *Journal of Sound and Vibration*, **330**(10): 2185–2200.

Bahar A, Pozo F, Acho L, Rodellar J and Barbat A (2010), "Hierarchical Semi-active Control of Base-isolated Structures Using a New Inverse Model of Magnetorheological Dampers," *Computers and Structures*, **88**(7–8): 483–496.

Bharti SD, Dumne SM and Shrimali MK (2014), "Earthquake Response of Asymmetric Building with MR Damper," *Earthquake Engineering and Engineering Vibration*, **13**: 305–316.

Casciati F, Rodellar J and Yildirim U (2012), "Active and Semi-active Control of Structures–Theory and Applications: A Review of Recent Advances," *Journal of Intelligent Material Systems and Structures*, **23**(11): 1181–1195.

Castellano MG, Colato GP and Infanti S (2004), "Use of Viscous Dampers and Shock Transmission Units in the Seismic Protection of Buildings," *Proceedings of the 13th World Conference on Earthquake Engineering*, Vancouver, B. C., Canada, Paper No. 2174.

Chopra AK (1995), *Dynamics of Structures: Theory and Applications to Earthquake Engineering (2nd ed)*, Prentice-Hall, New York.

Chu SY, Soong TT and Reinhorn AM (2005), *Active, Hybrid and Semi-Active Structural Control – A Design and Implementation Handbook*, John Wiley & Sons Ltd., Chichester.

Dyke SJ and Spencer Jr. BF (1997), "A Comparison of Semiactive Control Strategies for the Magnetorheological Dampers," *Proceedings of the International Conference on Intelligent Information Systems* (*IIS '97*), Grand Bahama Island, Bahamas, pp. 580–584.

Gattulli V, Lepidi M and Potenza F (2009), "Seismic Protection of Frame Structures via Semi-active Control: Modeling and Implementation Issues," *Earthquake Engineering and Engineering Vibration*, **8**: 627–645.

Gavin HP and Aldemir U (2005), "Optimal Control of Earthquake Response Using Semiactive Isolation," *Journal of Engineering Mechanics*, ASCE, **131**(8): 769–776.

Ikeda Y (2009), "Active and Semi-active Vibration Control of Buildings in Japan–Practical Applications and Verification," *Structural Control and Health Monitoring*, **16**(7–8): 703–723.

Isidori A (1995), *Nonlinear Control Systems–Volume 1 (3rd ed)*, Springer-Verlag, London.

Jansen LM and Dyke SJ (2000), "Semi-active Control Strategies for MR Dampers: A Comparative Study," *Journal of Engineering Mechanics*, ASCE, **126**(8): 795–803.

Jung H, Min Choi K, Spencer Jr. BF and Lee I (2006), "Application of Some Semi-active Control Algorithms to a Smart Base-isolated Building Employing MR

Dampers," *Structural Control and Health Monitoring*, **13**(2–3): 693–704.

Komatsu H, Shinozaki Y, Sanui Y, Maseki R, Yoshida K, Kitagawa Y, Toyama J and Nagashima I (2007), "A Building with Semi-active Base Isolation Using Sliding Mode Control," *Proceedings of SMSST'07, World Forum on Smart Materials and Smart Structures Technology*, Chongqing & Nanjing, China, pp. 523–524.

Luo N, Rodellar J, Vehí J and De la Sen M (2001), "Composite Semiactive Control of a Class of Seismically Excited Structures," *Journal of the Franklin Institute*, **338**(2–3): 225–240.

Maciejowski J (2002), *Predictive control with constraints*, Pearson Education Limited, Essex.

Mehrparvar B and Khoshnoudian T (2012), "Performance-based Semi-active Control Algorithm for Protecting Base Isolated Buildings from Near-fault Earthquakes", *Earthquake Engineering and Engineering Vibration*, **11**: 43–55.

NP EN 1998–1 (2010), *Eurocode 8–1: Design of Structures for Earthquake Resistance, Eurocodigo8, Projecto de Estruturas para Resistência aos Sismos – Parte1: Regras Gerais, Acções Símicas e Regras para Edifícios*, Instituto Português da Qualidade, Caparica.

Ogata K (1970), *Modern Control Engineering*, Prentice-Hall Inc., Englewood Cliffs.

Ou Jinping and Li Hui (2009), "Design Approaches for Active, Semi-active and Passive Control Systems Based on Analysis of Characteristics of Active Control Force," *Earthquake Engineering and Engineering Vibration*, **8**: 493–506.

Preumont A (2002), *Vibration Control of Active Structures—An Introduction* (*2nd ed*), Kluwer Academic Publishers, Dordrecht.

Qin X, Zhang X and Sheldon C (2008), "Study on Semi-active Control of Mega-sub Controlled Structure by MR Damper Subject to Random Wind Loads," *Earthquake Engineering and Engineering Vibration*, **7**: 285–294.

Rodríguez A, Pozo F, Bahar A, Acho L, Vidal Y and Rodellar J (2012), "Force-derivative Feedback Semi-active Control of Base-isolated Buildings Using Large-scale MR Fluid Dampers," *Structural Control and Health Monitoring*, **19**(1): 120–145.

Sadek F and Mohraz B (1998), "Semiactive Control Algorithms for Structures with Variable Dampers," *Journal of Engineering Mechanics*, ASCE, **124**(9): 981–990.

Shook D, Lin P, Lin T and Roschke PN (2007), "A Comparative Study in the Semi-active Control of Isolated Structures," *Smart Materials and Structures*, **16**(4): 1433–1446.

Skogestad S and Postlethwaite I (1996), *Multivariable Feedback Control—Analysis and Design*, John Wiley & Sons Ltd., Chichester.

Soong TT and Dargush GF (1997), *Passive Energy Dissipation Systems in Structural Engineering*, John Wiley & Sons Ltd., Chichester.

Soong TT and Spencer Jr. BF (2002), "Supplemental Energy Dissipation: State-of-the-art and State-of-the Practice," *Engineering Structures*, **24**(3): 243–259.

Spencer Jr. BF (2008), "Structural Control in Honor of Takuji Kobori," *Proceedings of the 14th World Conference on Earthquake Engineering*, Beijing, China.

Spencer Jr. BF and Nagarajaiah S (2003), "State of the Art of Structural Control," *Journal of Structural Engineering*, ASCE, **129**(7): 845–856.

Symans MD and Constantinou MC (1995), "Development and Experimental Study of Semi-active Fluid Damping Devices for Seismic Protection of Structures," *National Center for Earthquake Engineering Research* (NCEER), Buffalo, Report No. 95–0011.

Symans MD and Constantinou MC (1999), "Semi-active Control Systems for Seismic Protection of Structures: a State-of-the-art Review," *Engineering Structures*, **21**(6): 469–487.

Wang DH and Liao WH (2011), "Magnetorheological Fluid Dampers: a Review of Parametric Modeling," *Smart Materials and Structures*, **20**(2): 023001(34pp).

Zapateiro M, Karimi HR, Luo N and Spencer Jr. BF (2010), "Real-time Hybrid Testing of Semiactive Control Strategies for Vibration Reduction in a Structure with MR Damper," *Structural Control and Health Monitoring*, **17**(4): 427–451.